

# Design of omnidirectional asymmetrical high reflectors for optical telecommunication wavelengths

J. Zaghdoudi, M. Kanzari<sup>a</sup>, and B. Rezig

Laboratoire de Photovoltaïque et Matériaux Semi-conducteurs (LPMS), École Nationale d'ingénieurs de Tunis BP 37 Belvédère 1002 Tunis, Tunisia

Received 20 May 2004

Published online 14 December 2004 – © EDP Sciences, Società Italiana di Fisica, Springer-Verlag 2004

**Abstract.** A design for omnidirectional asymmetrical high reflectors for optical telecommunication wavelengths is described. Asymmetry was introduced by applying a power law, so that the coordinates  $y$  of the transformed object were determined through the coordinates  $x$  of the quarter-wave stack air/H(LH)<sup>15</sup>/air in accordance with the following rule  $y = x^{1+k}$ . Here  $k$  is the coefficient defining the asymmetry degree. It is shown that a high-reflection band at any incident angle for both polarizations, i.e., an omnidirectional high reflection band of 0.74  $\mu\text{m}$  for optical telecommunication wavelengths 0.85 and 1.3  $\mu\text{m}$  is found for the transformed system: air/Te(SiO<sub>2</sub>/Te)<sup>15</sup>/air corresponding to the optimized  $k$  value 0.24.

**PACS.** 42.70.Qs Photonic bandgap materials – 78.20.Bh Theory, models, and numerical simulation – 77.55.+f Dielectric thin films

## 1 Introduction

Over the past few years much effort has been devoted to the study of the propagation of electromagnetic (EM) waves in periodic dielectric structures [1,2]. The band gap structure of photonic crystals has been studied experimentally, numerically, and analytically. All of these studies confirmed the possibility of creating a complete gap in the frequency spectrum. Various applications of the omnidirectional high reflector as a one dimensional photonic band gap structure may be expected to improve the performance of photonic devices [3–6]. It is important to notice that the most results obtained for 1D, 2D and 3D structures are obtained by means of these numerical methods and others developed to this end. However, the few analytical studies performed to date concerned only the low dimensional photonic crystals. Probably the first analytic work for the 1D Bragg scattering system, a number of theoretical and experimental papers reporting studies in the far field transmission have been published, with emphasis placed on the occurrence of the photonic band gap (PBG). However only a few studies have been made on the field of near field optics, with emphasis on what really happens in the middle of this photonic structure. It is well known that quarter-wave optical thickness multi-layer stacks with alternant low- and high-refractive index dielectric layers are widely used as high reflectors in a limited range of wavelengths and incident angles [7]. The deviations of periodic multilayer structures from perfect ones are an important problem in optics since the

structure of real multilayer systems differs from the ideal periodic multilayer structures.

The purpose of this research consists in searching for a possibility for asymmetry of one dimensional periodic multilayer structure with a controlled asymmetry to be evaluated optically. Asymmetry was introduced by applying a power law, so that the coordinates  $y$  of the transformed object were determined through the coordinates  $x$  of the initial (periodic structure) object in accordance with the following rule:

$$y = x^{1+k}$$

Here  $k$  is the coefficient defining the asymmetry degree. So for example, the periodic structure is projected into itself without any changes of dimension, if  $k = 0$ . Deviation of the magnitude of  $k$  from zero leads to an asymmetry appearing in the transformed periodic multilayer structure. The aim of this work is to study the effect of this asymmetry on the optical reflection properties of the transformed periodic multilayer structure.

## 2 Method

The method that we introduce here for calculating the intensity of the electric field is based on Abele's method [8] in terms of forward and backward propagating electric fields, that is,  $E^+$  and  $E^-$ , which were introduced to calculate the reflection and transmission.

Abeles showed that the relation among the amplitudes of the electric fields of the incident wave  $E_0^+$ , reflected

<sup>a</sup> e-mail: mounir.kanzari@ipeit.rnu.tn

wave  $E_0^-$ , and transmitted wave after  $m$  layers  $E_{m+1}^+$  is expressed as the following matrix for stratified films within  $m$  layers.

$$\begin{pmatrix} E_0^+ \\ E_0^- \end{pmatrix} = \frac{C_1 C_2 C_3 \dots C_{m+1}}{t_1 t_2 t_3 \dots t_{m+1}} \begin{pmatrix} E_{m+1}^+ \\ E_{m+1}^- \end{pmatrix}. \quad (1)$$

Here,  $C_j$  is the propagation matrix with the matrix elements.

$$C_j = \begin{pmatrix} \exp(-i\phi_{j-1}) & r_j \exp(-i\phi_{j-1}) \\ r_j \exp(i\phi_{j-1}) & \exp(-i\phi_{j-1}) \end{pmatrix} \quad (2)$$

where  $t_j$  and  $r_j$  are the Fresnel transmission and reflection coefficients, respectively, between the  $(j-1)$ th and  $j$ th layer.

The Fresnel coefficients  $t_j$  and  $r_j$  can be expressed as follows by using the complex refractive index  $\hat{n}_j = n_j + ik_j$  and the complex refractive angle  $\theta_j$ : for parallel (P) polarisation:

$$r_{jp} = \frac{\hat{n}_{j-1} \cos \theta_j - \hat{n}_j \cos \theta_{j-1}}{\hat{n}_{j-1} \cos \theta_j + \hat{n}_j \cos \theta_{j-1}} \quad (3)$$

$$t_{jp} = \frac{2\hat{n}_{j-1} \cos \theta_{j-1}}{\hat{n}_{j-1} \cos \theta_j + \hat{n}_j \cos \theta_{j-1}}. \quad (4)$$

Moreover, for perpendicular (s) polarisation:

$$r_{js} = \frac{\hat{n}_{j-1} \cos \theta_{j-1} - \hat{n}_j \cos \theta_j}{\hat{n}_{j-1} \cos \theta_{j-1} + \hat{n}_j \cos \theta_j} \quad (5)$$

$$t_{js} = 2 \frac{\hat{n}_{j-1} \cos \theta_{j-1}}{\hat{n}_{j-1} \cos \theta_{j-1} + \hat{n}_j \cos \theta_j}. \quad (6)$$

The complex refractive indices and the complex angles of incidence obviously follow Snell's law:  $\hat{n}_{j-1} \sin \theta_{j-1} = \hat{n}_j \sin \theta_j$  ( $j = 1, 2, \dots, m+1$ ). The values  $\phi_{j-1}$  in equation (2) indicate the change in the phase of the wave between the  $(j-1)$ th and  $j$ th boundaries and are expressed by the equation available for  $j < 1$

$$\phi_0 = 0 \quad (7)$$

$$\phi_{j-1} = \frac{2\pi}{\lambda} \hat{n}_{j-1} d_{j-1} \cos \theta_{j-1}, \quad (8)$$

where  $\lambda$  is the wavelength of the incident light in vacuum and  $d_{j-1}$  indicates the thickness of the  $(j-1)$ th layer.

By putting  $E_{m+1}^- = 0$ , because there is no reflection from the final phase, Abeles [8] obtained a convenient formula for the total reflection and transmission coefficients, which correspond to the amplitude reflectance  $r$  and transmittance  $t$ , respectively, as follows:

$$r = \frac{E_0^-}{E_0^+} = \frac{c}{a} \quad (9)$$

$$t = \frac{E_{m+1}^+}{E_0^+} = \frac{t_1 t_2 \dots t_{m+1}}{a}. \quad (10)$$

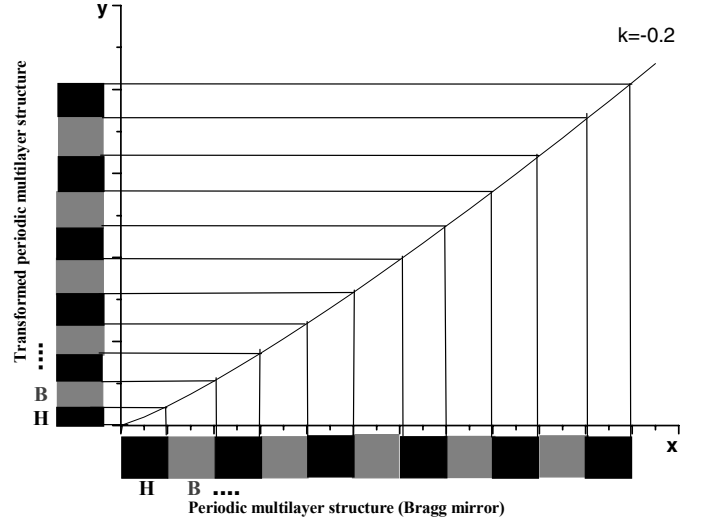


**Fig. 1.** Principle of introducing an asymmetry into the one dimensional periodic multilayer system: Transformation of a perfect one dimensional periodic multilayer system into an asymmetric one, for example for  $k = -0.2$ .

The quantities  $a$  and  $c$  are the matrix elements of the product of all  $C_j$  matrix:

$$C_1 C_2 C_3 \dots C_{m+1} = \begin{pmatrix} a & b \\ c & d \end{pmatrix}. \quad (11)$$

By using equations (9) and (10), we can easily obtain energy reflectance  $R$  as:

$$R = |r|^2 \quad (12)$$

for both polarisation, and the energy transmittance  $T$  as:

$$T_s = \text{Re} \left( \frac{\hat{n}_{m+1} \cos \theta_{m+1}}{\hat{n}_0 \cos \theta_0} \right) |t_s|^2 \quad (13)$$

$$\begin{aligned} T_p &= \text{Re} \left( \frac{\cos \theta_{m+1} / \hat{n}_{m+1}}{\cos \theta_0 / \hat{n}_0} \right) \left| \frac{\hat{n}_{m+1}}{\hat{n}_0} t_s \right|^2 \\ &= \text{Re} \left( \frac{\hat{n}_{m+1} \cos \theta_{m+1}}{\hat{n}_0 \cos \theta_0} \right) |t_p|^2 \end{aligned} \quad (14)$$

for  $s$  and  $p$  polarisation, respectively, where  $\text{Re}$  indicates the real part.

The asymmetry was introduced by applying a power law, so that the coordinates  $y$  which represent the transformed object were determined using the coordinates  $x$  of the initial object in accordance with the following rule:

$$y = x^{1+k}.$$

Here  $k$  is the coefficient defining the asymmetry degree. Figure 1 shows the principle of introducing asymmetry into the periodic structure.

The initial optical phase thickness when we apply the  $y$  function is:

$$\phi = \frac{2\pi}{\lambda} n d \cos \theta$$

which takes the following form:

$$\phi_j = \frac{2\pi}{\lambda} x_0 \left( j^{k+1} - (j-1)^{k+1} \right) \cos \theta_j.$$

Here  $j$  designates the  $j$ th layer and  $x_0 = \frac{\lambda_0}{4}$  is the optical thickness of the each layer of the periodic structure with the reference wavelength  $\lambda_0 = 0.5 \mu\text{m}$ . For the transformed system, the optical thickness of each layer becomes variable and depends on the  $j$ th layer and  $k$  the coefficient defining the asymmetry degree. So, the optical thickness of each layer after transformation by the  $y$  function takes the following form:

$$x'_{0j} = x_0 \left( j^{k+1} - (j-1)^{k+1} \right) \text{ for } j \geq 1.$$

In the following numerical investigation, we chose firstly  $\text{SiO}_2$  (L) and  $\text{TiO}_2$  (H) as two elementary layers, with refractive indices  $n_L = 1.45$  and  $n_H = 2.3$ , respectively. Secondly we chose  $\text{SiO}_2$  (L) and Te (H) as two elementary layers, with refractive indices  $n_L = 1.45$  and  $n_H = 4.6$ , respectively. For our study, all the regions are assumed to be linear, homogeneous, non absorbing, and with no optical activity in the spectral region  $[0.2-2] \mu\text{m}$ .

Here, we study the optical reflection properties in the spectral range  $[0.2-2] \mu\text{m}$  of the transformed system  $\text{H}(\text{LH})^{15}$  by the  $y$  function as described by Figure 1. The value 15 of the periodical (LH) corresponds to the minimal (LH) number which can be traced to have a photonic band gap with maximal reflectance of about 100%. We note that from the value 15 of the periodical (LH), no considerable improvement in the performances of the systems is observed.

It is clear that for a given value of  $k$ , the periodic system becomes deformed and the thickness of each layer increases with increasing  $k$ .

### 3 Results and discussion

#### 3.1 $\text{TiO}_2/\text{SiO}_2$ system

The reflectances  $R$  at normal incidence of a transformed quarter-wave stack  $\text{air}/\text{H}(\text{LH})^{15}/\text{air}$  by the  $y$  function are shown in Figure 2, as a function of wavelength and the parameter  $k$ . The reference wavelength is  $\lambda_0 = 0.5 \mu\text{m}$  and the parameter  $k$  is chosen to vary between  $-0.2$  and  $0.316$  for which the photonic band gap does not exceed the spectral range  $[0.2-2] \mu\text{m}$ . As the parameter  $k$  increases, the center wavelengths of the photonic band gaps shift to the higher wavelength region as shown in Figure 3 and the reflection bandwidth is broader for the high values of  $k$  as we can see from Figure 4. We then thought to use the transformed stack as omnidirectional high-reflecting mirror in the spectral range  $[1-2] \mu\text{m}$ , which generates the telecommunication wavelength  $1.55 \mu\text{m}$ . In Figures 5 we represent the reflectances for both polarisation parallel (P) and perpendicular (S) for  $k = 0.316$  for which the photonic band gap is broader. The S-reflection bandwidth is broader than at normal incidence, whereas the P-reflection bandwidth is

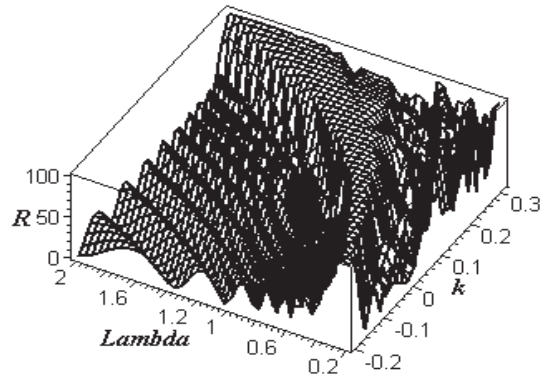


**Fig. 2.** Reflectances of a quarter-wave stack of the transformed  $\text{TiO}_2/\text{SiO}_2$  system at normal incidence as a function of wavelength and asymmetry degree  $k$  in the spectral range  $[0.2-2] \mu\text{m}$ .

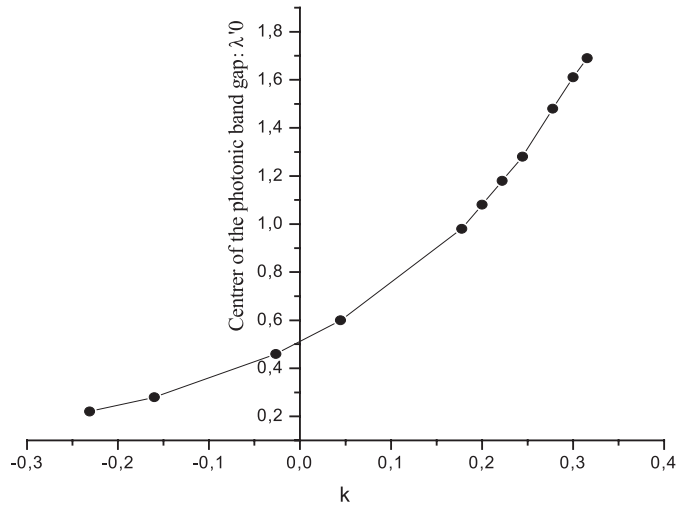


**Fig. 3.** The central wavelength of the photonic band gap of the transformed  $\text{TiO}_2/\text{SiO}_2$  system at normal incidence, as a function of the asymmetry degree  $k$  in the spectral range  $[0.2-2] \mu\text{m}$ .

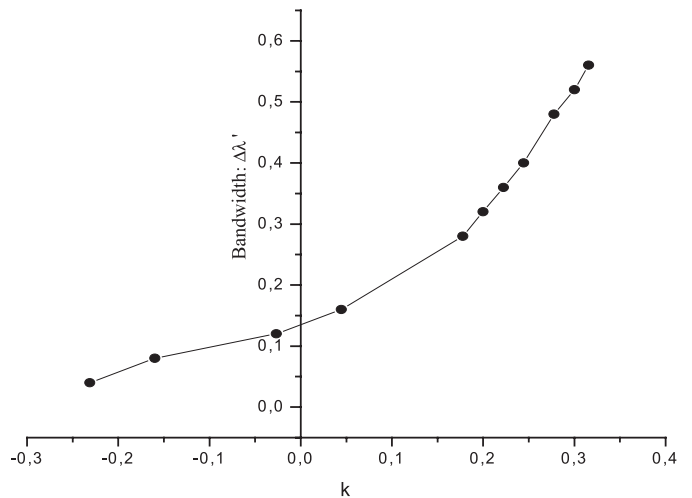


**Fig. 4.** Bandwidth of the photonic band gap of the transformed  $\text{TiO}_2/\text{SiO}_2$  system at normal incidence as a function of asymmetry degree  $k$  in the spectral range  $[0.2-2] \mu\text{m}$ .

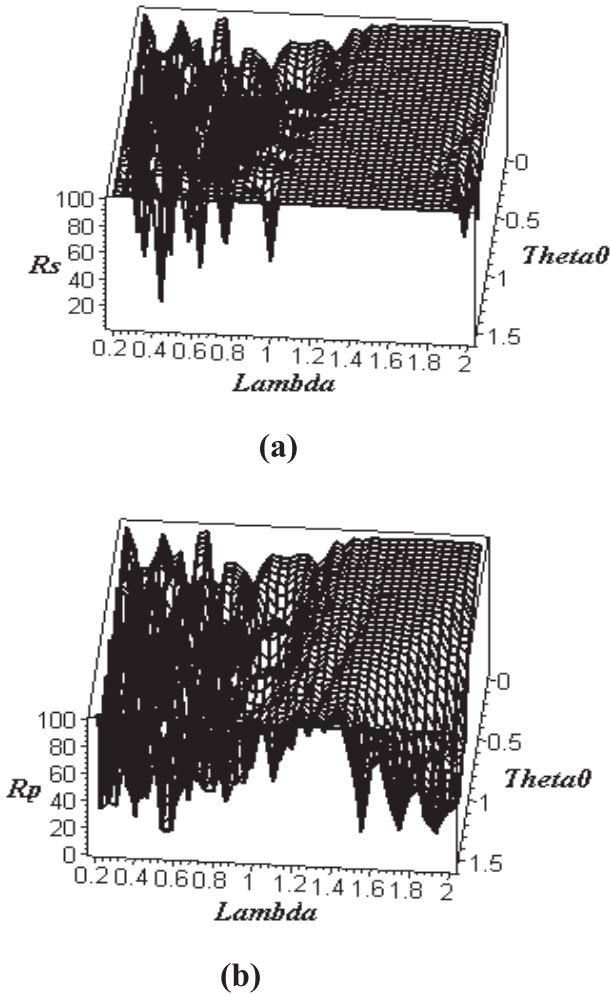


**Fig. 5.** Reflectances of a quarter-wave stack of the transformed  $\text{TiO}_2/\text{SiO}_2$  system as a function of wavelength and incident angle for the optimal asymmetric degree  $k = 0.316$  in the spectral range  $[0.2-2] \mu\text{m}$  (a) for S-polarized light (b) for P-polarized light.

narrower. The variation of  $\lambda_{\text{long}}(\theta_0)$  and  $\lambda_{\text{short}}(\theta_0)$  in both S- and P-reflection bands is shown in Figure 6 as a function of incident angle  $\theta_0$ . Note that a high reflection band at incidence angle below  $57^\circ$  exists for both polarizations and no omnidirectional high reflection band can be established for any incidence angle. Consequently, the transformed system by the  $y$  function for the system  $\text{TiO}_2/\text{SiO}_2$  exhibits i) for the telecommunication wavelength  $1.55 \mu\text{m}$  an omnidirectional high reflecting mirror only for incident angles below  $57^\circ$  and ii) present the advantage that the center wavelengths of the photonic band gaps shift to the higher wavelength region without changing the reference wavelength as reported in [6]. Furthermore, is it possible to extend the omnidirectional high-reflection bandwidth to cover the optical wavelength telecommunication  $1.55 \mu\text{m}$  for any incident angle? The solution resides in the choice of the high index layer. Indeed we chose tellurium as a layer of high refractive index of value 4.6. Examination of

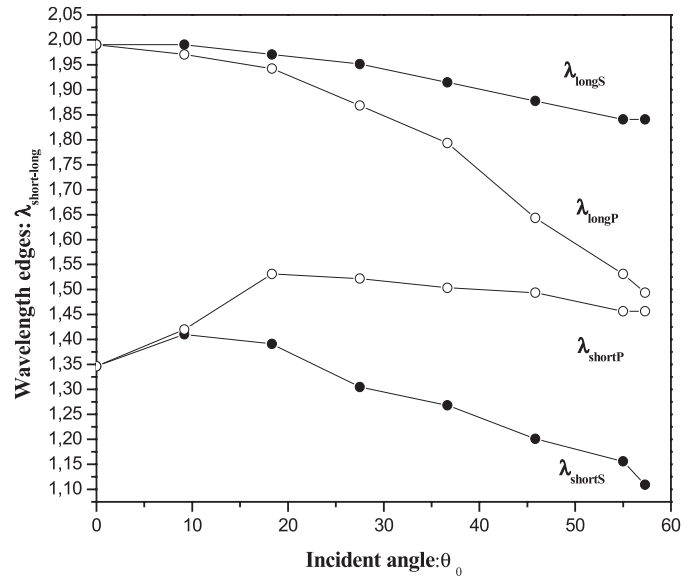


**Fig. 6.** Reflection band shift of the transformed  $\text{TiO}_2/\text{SiO}_2$  system as a function of incident angle for the optimal asymmetric degree  $k = 0.316$  in the spectral range  $[0.2-2] \mu\text{m}$ . The omnidirectional high-reflection band is obtained only for an incident angle less than  $57^\circ$ .

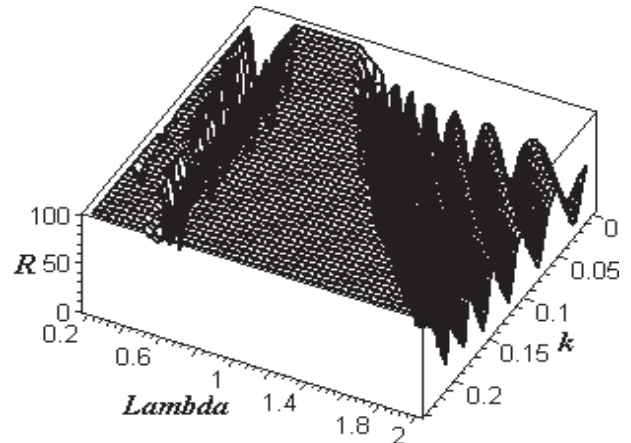
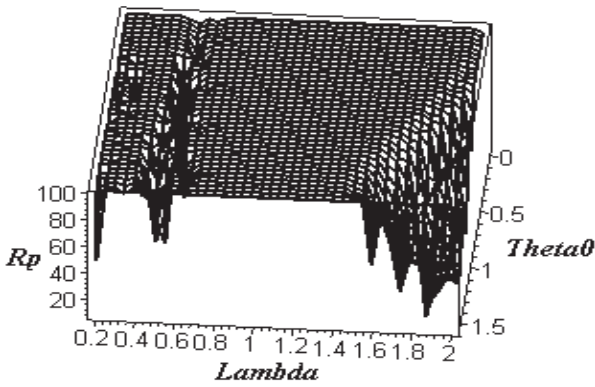


**Fig. 7.** Reflectances of a quarter-wave stack of the transformed  $\text{Te}/\text{SiO}_2$  system at normal incidence as a function of wavelength and asymmetric degree  $k$  in the spectral range  $[0.2-2] \mu\text{m}$ .

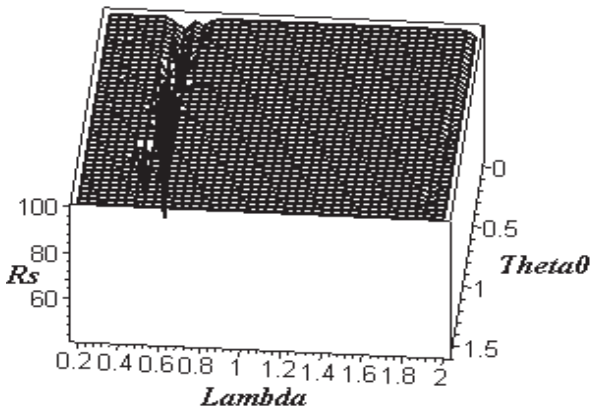
the transformation of the system  $\text{Te}/\text{SiO}_2$  permits us to reach our objectives.

### 3.2 $\text{Te}/\text{SiO}_2$ system

The reflectances  $R$  at normal incidence of a transformed quarter-wave stack  $\text{air}/\text{H}(\text{LH})^{15}/\text{air}$  by the  $y$  function are shown in Figure 7 as a function of wavelength and the parameter  $k$ . The reference wavelength is  $\lambda_0 = 0.5 \mu\text{m}$  and the parameter  $k$  is chosen to vary between 0 and 0.24 for which the photonic band gap does not exceed the spectral range  $[0.2-2] \mu\text{m}$ . We observed the same behavior for the displacement of the center wavelengths as well as



(a)



(b)

**Fig. 8.** Reflectances of a quarter-wave stack of the transformed Te/SiO<sub>2</sub> system as a function of wavelength and incident angle for the optimal asymmetry degree  $k = 0.24$  in the spectral range  $[0.2-2] \mu\text{m}$  (a) for P-polarized light (b) for S-polarized light.

the widening of the reflection bandwidth compared with the case  $n_H = 2.3$ . In Figure 8 we show the reflectances for both polarisation parallel (P) and perpendicular (S) for  $k = 0.24$  for which the photonic band gap is broader. The S-reflection bandwidth is broader than at normal incidence, whereas the P-reflection bandwidth is narrower. The variation of  $\lambda_{long}(\theta_0)$  and  $\lambda_{short}(\theta_0)$  in both S- and P-reflection bands is shown in Figure 9 as a function of incident angle  $\theta_0$  for the optimized  $k$  value 0.24. As long as  $\lambda_{long}^P(90^\circ)$  is larger than  $\lambda_{short}(0^\circ)$ , a high-reflection band at any incident angle for both polarizations, i.e., an omnidirectional high reflection band of  $0.74 \mu\text{m}$ , exists between  $\lambda_{short}(0^\circ)$  and  $\lambda_{long}^P(90^\circ)$ . Consequently, the omnidirectional high-reflection bandwidth covers the optical wavelength telecommunications  $0.85$  and  $1.3 \mu\text{m}$ . It is interesting to note that this result is impossible to reach for the system not transformed by the  $y$  function as shown in

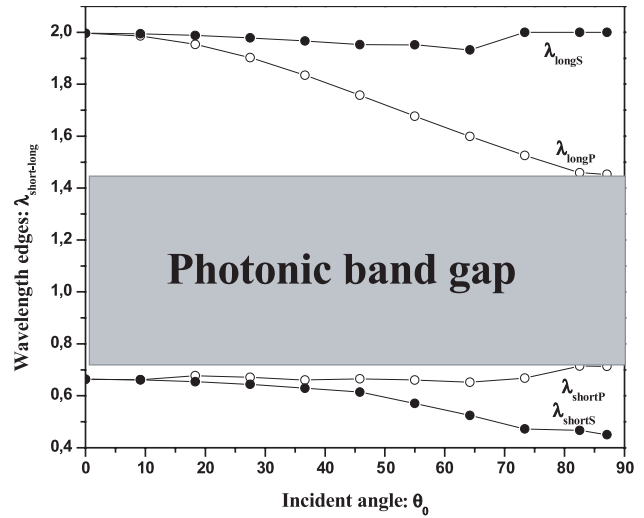


**Fig. 9.** Reflection band shift of the non transformed Te/SiO<sub>2</sub> system as a function of incident angle for the optimal asymmetry degree  $k = 0.24$  in the spectral range  $[0.2-2] \mu\text{m}$ . The dashed area represents the omnidirectional high-reflection band.

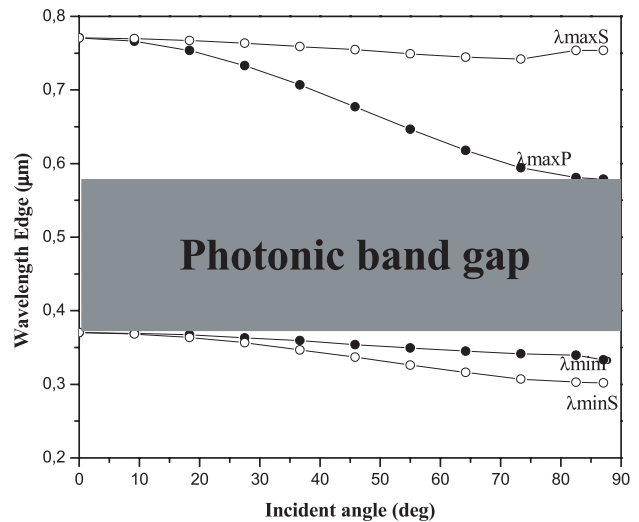


**Fig. 10.** Reflection band shift of the non transformed Te/SiO<sub>2</sub> system (periodic system) as a function of incident angle corresponding to the asymmetry degree  $k = 0$  in the spectral range  $[0.2-2] \mu\text{m}$ . The dashed area represents the omnidirectional high-reflection band.

Figure 10 for the case  $k = 0$ . Indeed, the omnidirectional high-reflection bandwidth of  $0.4 \mu\text{m}$ , does not covers the optical wavelength telecommunications which are known to be  $0.85$ ,  $1.3$  and  $1.55 \mu\text{m}$ .

### Conclusion

We have studied the reflection-band of the transformed quarter-wave multilayer systems air/H(LH)<sup>15</sup>/air by the function  $y = x^{1+k}$ , where the coordinates  $y$  which represent the transformed object were determined through the

coordinates  $x$  of the initial object. In the following numerical investigation, we chose firstly  $\text{SiO}_2$  (L) and  $\text{TiO}_2$  (H) as two elementary layers, with refractive indices  $n_L = 1.45$  and  $n_H = 2.3$  and secondly we chose  $\text{SiO}_2$  (L) and Te (H) as two elementary layers, with refractive indices  $n_L = 1.45$  and  $n_H = 4.6$ . The results show that a high-reflection band at any incident angle for both polarizations, i.e., an omnidirectional high reflection band of  $0.74 \mu\text{m}$  for optical telecommunication wavelengths  $0.85$  and  $1.3 \mu\text{m}$  is found only for the transformed system:  $\text{air/Te}(\text{SiO}_2/\text{Te})^{15}/\text{air}$  corresponding to the optimized  $k$  value  $0.24$ . The advantage of this work over previous studies is the necessity for only 15 periods (LH) and a reference wavelength  $\lambda_0 = 0.5 \mu\text{m}$  to reach our objectives. In the previous work [6] 30 to 40 periods (LH) and a reference wavelength  $\lambda_0 = 1.8102 \mu\text{m}$  are used to reach the same objectives. In summary, we have proposed a simple figure of merit that allows for an improvement in the performance of omnidirectional reflectors, especially when the number

of periods is not too large by comparison with previous studies.

## References

1. Y. Fink, J.N. Winn, S. Fan, C. Chen, J. Michel, J.D. Joannopoulos, E.L. Thomas, *Science* **282**, 1679 (1998)
2. J.P. He, L.F. Shen, S.S. Xiao, S.L. He, *Chin. Phys. Lett.* **19**, 69 (2002)
3. K.M. Chen, A.W. Sparks, H.-C. Luan, D.R. Lim, K. Wada, L.C. Kimerling, *Appl. Phys. Lett.* **75**, 3805 (1999)
4. G.V. Morozov, R. Gr. Maev, G.W.F. Drake, *Phys. Rev. E* **60**, 4860 (1999)
5. M. Ibanescu, Y. Fink, S. Fan, E.L. Thomas, J.D. Joannopoulos, *Science* **289**, 415 (2000)
6. S.H. Kim, C.K. Hwangbo, *Applied Optics* **41**, 3187 (2002)
7. W.H. Southwell, *Applied Optics* **38**, 5464 (1999)
8. F. Abelès, *Ann. Phys. Paris* **12**, 596 (1950)